CONSORTIUM for BUILDING ENERGY INNOVATION

Project 2.5 – Virtual Sensing Automation, Demonstration, and Assessment
M/GN number: M2.5.b

Project Objective: The goal of this project is to develop, demonstrate, and evaluate hardware and software implementations of virtual sensors for RTUs.
Objective/goal of this Milestone or Go/No-Go decision point and evaluation criteria: Description: Document implementation of virtual sensors within a low-cost microprocessor Verification: Report to CBEI describing implementation
Major findings/Result: A virtual sensor system (compatible with the VOLTTRON platform) has been designed and an initial prototype has been tested. The overall architecture of the virtual sensor system has been described including the data acquisition components and virtual sensor models. Initial prototype hardware has been designed that measures all required sensor inputs and is capable of running all software implementations. The software implementation has been described as well as future testing and evaluation plans to characterize the performance for different systems. Preliminary test results characterizing the virtual refrigerant charge sensor accuracy have also been described.
Contributors: Purdue – Andrew Hjortland, Jim Braun, Orkan Kurtulus, Akash Patil

Date: Dec. 31, 2015

CONSORTIUM for BUILDING ENERGY INNOVATION

CONTENTS

1. Introduction

1.1. Project Motivation and Objectives

Studies have shown that RTUs tend to be poorly maintained and significant energy may be wasted annually due to unnoticed or unrepaired equipment faults. Previous work on FDD for HVAC systems has yielded positive results and potential for significant energy and utility cost savings by identifying faults in these systems sooner. This is especially true of virtual sensor based FDD protocols due to the ability to detect and diagnose multiple faults simultaneously.

Despite the promising results obtained by previous work on FDD, manufacturers have been slow to incorporate FDD technologies for a few reasons:

- FDD systems must be low-cost and easy to install,
- uncertainty with respect to economic benefit/savings potential still exists,
- and lack of integration and interoperability with other building technologies.

In order to address these issues, a suite of virtual sensors have been designed and implemented using a low-cost microprocessor with four direct temperature (or pressure) measurements. These virtual sensors include the virtual refrigerant charge sensor, virtual cooling capacity sensor, and virtual COP sensor. The designed system includes plans for all hardware requirements, as well as all software requirements. Ultimately, this virtual sensor package can be integrated within a RTU FDD system to provide an extensive fault detection and diagnostics capability.

1.2. Virtual Sensor based RTU FDD Background

Recent research has provided evidence that fault detection sensitivity and fault diagnosis accuracy of fault detection and diagnostics (FDD) methodologies can be improved when accurate virtual sensor technologies are incorporated without adding significant instrumentation costs. One advantage of virtual sensors is the ability to estimate physical quantities that may be too expensive to measure directly. Furthermore, some quantities like the amount of refrigerant charge contained in a direct-expansion (DX) air-conditioning system are impossible to measure directly while the unit is in operation. Previous work has shown units that are undercharged tend to have less available cooling capacity and tend to operate with lower efficiency. One additional advantage of virtual sensors is the ability to decouple HVAC equipment components so that different virtual sensors are only sensitive to a single fault. This enables accurate fault diagnoses even when multiple faults affect a system simultaneously.

Virtual Refrigerant Charge Sensor

Previous work has shown that the amount of refrigerant charge contained in a system can be estimated using measurements of the compressor suction superheat and liquid-line subcooling. The compressor suction superheat, ΔT_{sh}, is equal to the temperature difference defined by Equation (1.1)

$$\Delta T_{sh} = T_{suc} - T_{eri} \tag{1.1}$$

where T_{suc} is the refrigerant temperature at the compressor inlet (suction) and T_{eri} is the temperature of the refrigerant entering the evaporator (a measure of saturation temperature). The liquid-line subcooling, ΔT_{sc}, is calculated using a similar temperature difference, given by Equation (1.2),

$$\Delta T_{sc} = T_{crs} - T_{cro} \tag{1.2}$$

where T_{crs} is the refrigerant saturation temperature in the condenser and T_{cro} is the refrigerant temperature at the condenser outlet. The amount of refrigerant charge in a DX system relative to the normal amount can be estimated using a virtual refrigerant charge sensor. The functional form of this sensor is given by Equation (1.3)

$$\frac{m_{\text{actual}}}{m_{\text{normal}}} = 1 + k_{sh}\left(\Delta T_{sh} - \Delta T_{sh,rated}\right) + k_{sc}\left(\Delta T_{sc} - \Delta T_{sc,rated}\right) + k_x\left(x_{eri} - x_{eri,rated}\right) \tag{1.3}$$

where $\Delta T_{sh,rated}$, $\Delta T_{sc,rated}$, and $x_{eri,rated}$ are the superheat, subcooling, and evaporator refrigerant inlet quality of a properly charged system at the rating condition respectively. Equation (1.3) also requires three empirical parameters: k_{sh}, k_{sc}, k_x. Determining these empirical parameters using performance data collected in an open laboratory space was described previously in Project 2.5 Milestone Report A.

The correlation defined by Equation (1.3) requires measurements of the thermodynamic quality of the refrigerant entering the evaporator. Since it is impossible to measure the thermodynamic quality directly, the use of thermodynamic property relations and a commonly used vapor-compression cycle assumption must be used to estimate this quantity. Commonly, the expansion process of the vapor compression cycle is assumed to be isenthalpic; the enthalpy at the inlet and outlet of the expansion valve is constant,

$$h_{cro} = h_{eri}. \tag{1.4}$$

With this assumption, the thermodynamic quality at the evaporator inlet, x_{eri}, can be calculated using thermodynamic property relations if the condenser outlet enthalpy is known and the evaporator inlet temperature is measured,

$$x_{eri} = f(T_{eri}, h_{eri} = h_{cro}). \tag{1.5}$$

To calculate the enthalpy of the enthalpy of the refrigerant exiting the condenser, thermodynamic property relations can be used when nonzero subcooling exists using the outlet temperature and the condenser saturation temperature.

Virtual Compressor Power Sensor

Some faults, especially faults reducing the condenser airflow or heat transfer coefficient like fouling, have a significant impact on the instantaneous power drawn by the compressor. An FDD algorithm can detect these problems when abnormal power is drawn by the system. While direct measurements of

compressor power are available, these are relatively expensive when compared with the typical cost of a RTU. A virtual compressor power sensor has been developed using low-cost temperature measurements as an alternative to direct power sensor measurements.

This virtual sensor is essentially a performance mapping of the compressor power under different operating conditions. These mappings are actually available for all compressors used in air-conditioning applications since it is required by the Air-Conditioning, Heating, and Refrigeration Institute (AHRI), a certification organization. This means no additional laboratory tests are required to train empirical parameters since compressor manufacturers must perform them and make the results available. A 10-coefficient polynomial equation is used to relate the compressor suction saturation temperature, T_{ers}, and the compressor discharge saturation temperature, T_{crs}, to the compressor power requirement, $\dot{W}_{map}$,

$$\begin{aligned}\dot{W}_{map} = a_0 + \\ a_1 T_{ers} + a_2 T_{crs} + \\ a_3 T_{ers}^2 + a_4 T_{ers} T_{crs} + a_5 T_{crs}^2 + \\ a_6 T_{ers}^3 + a_7 T_{ers}^2 T_{crs} + a_8 T_{ers} T_{crs}^2 + a_9 T_{crs}^3\end{aligned} \quad (1.6)$$

where $a_{0\ldots9}$ are empirical coefficients that can be obtained from a manufacturer's data sheet. When a compressor with multiple stages is used on the system, a set of empirical coefficients are required for each stage of operation. To evaluate the compressor map given by Equation (1.6), measurements of two-phase refrigerant temperature in the evaporator and condenser can be used (evaporator inlet and a condenser return bend temperature). If direct measurements of the saturation temperatures are not possible, suction and discharge pressure transducers can be used to calculate these saturation temperatures since pressure and temperature are dependent properties within the two-phase dome.

Virtual Refrigerant Mass Flow Rate Sensor

Another important and useful quantity that can be leveraged by FDD algorithms is the system refrigerant mass flow rate. The mass flow rate of refrigerant within the system is impacted by many faults and reductions in mass flow rate can lead to reductions in cooling capacity and cycle efficiency. Along with compressor power, AHRI also requires rating the mass flow rate through a compressor at different operating conditions. As before, a 10-coefficient polynomial correlation in terms of T_{ers} and T_{crs} are required by manufacturers to relate the mass flow rate, $\dot{m}_{map}$,

$$\begin{aligned}\dot{m}_{map} = a_0 + \\ a_1 T_{ers} + a_2 T_{crs} + \\ a_3 T_{ers}^2 + a_4 T_{ers} T_{crs} + a_5 T_{crs}^2 + \\ a_6 T_{ers}^3 + a_7 T_{ers}^2 T_{crs} + a_8 T_{ers} T_{crs}^2 + a_9 T_{crs}^3\end{aligned} \quad (1.7)$$

where $a_{0\ldots9}$ are empirically determined coefficients. One limitation using Equation (1.7) to estimate refrigerant mass flow rate in practice is related to the superheat used when determining the empirical

parameters. During the testing, superheat is held at a constant value. Unfortunately, this is not the case in an actual system, where variations in superheat are likely due to different expansion devices, ambient conditions, and charge levels. An additional adjustment must be made to the performance map output to account for differences between the actual suction superheat and the superheat maintained during the ratings process. A correlation is given by Dabiri and Rice (1981) to account for variations in actual suction superheat during actual compressor operation,

$$\dot{m}_{ref} = \left[1 + F\left(\frac{\rho_{rated}}{\rho_{actual}} - 1\right)\right]\dot{m}_{map} \tag{1.8}$$

where ρ_{actual} and ρ_{rated} are measurements of the actual and rated suction density and F is an empirical parameter usually set to 0.75. In order to determine the actual suction density, thermodynamic property relations are used along with measurements of the compressor suction state.

Virtual Cooling Capacity Sensor

Perhaps the most important impact on system performance that a fault has on an air-conditioning system is the impact on cooling capacity. When total cooling capacity is reduced, the system must run longer to meet a given load and consume more energy. Furthermore, if cooling capacity is reduced sufficiently, the air conditioner may not have enough capacity during times of high loads. To estimate the cooling capacity of an air-conditioning system, a virtual cooling capacity sensor has been proposed that relies on state point measurements at the inlet and outlet of the evaporator, as well as the refrigerant mass flow rate. By calculating the enthalpy at the evaporator inlet, h_{eri}, and the compressor suction, h_{suc}, the cooling capacity can be calculated using Equation (1.9),

$$\dot{Q}_{cool} = \dot{m}_{ref}(h_{suc} - h_{eri}) \tag{1.9}$$

where $\dot{m}_{ref}$ is the mass flow rate of refrigerant in the system (given by the virtual refrigerant mass flow rate sensor). Using Equation (1.9) along with a properly tuned FDD algorithm enables detection of faults that impact cooling capacity.

Virtual COP Sensor

A final measure of system performance for an air conditioning system is the coefficient of performance (COP), which is the ratio of total cooling capacity to total power consumption. This performance metric is effectively the efficiency of the system, which can be calculated at any time during operation. Because of this, it is convenient to have an estimate of the current system COP within a FDD tool. Equation (1. 10) describes a virtual sensor for COP in terms of the virtual cooling capacity and virtual compressor power sensors.

$$\mathrm{COP} = \frac{\dot{Q}_{cool}}{\dot{W}_{map}} \tag{1. 10}$$

By using the virtual COP sensor as part of a FDD package, degradation in cooling cycle performance can be measured and faults impacting system efficiency can be detected.

2. Description of Virtual Sensor Hardware

Due to the limited availability of sensors installed on existing RTUs in production and the relatively modest computing resources available, additional electronics hardware is required to implement the virtual sensor package proposed in this work. The following section details the electronics designed to demonstrate the complete performance of the virtual sensor system: from data acquisition to calculation of virtual sensor outputs. The system designed can be considered standalone. These electronics can be installed on a typical RTU and with the proper initial configuration, an effective virtual sensor system can be utilized by building operators without any other sensor requirements or hardware. While this system could seemingly be applied as a retrofit, it was primarily designed from the standpoint of being embedded by equipment manufacturers during the production process.

2.1 Data Acquisition and Compute System

Sensor Inputs

In order to implement the virtual sensor models, four refrigerant-side temperature measurements (shown in Table 2.1) are required. Using only these refrigerant-side temperature sensors, all of the previously described virtual sensors can be implemented. This includes the virtual refrigerant charge (VRC) sensor, the virtual refrigerant mass flow rate (VRMF) sensor, the virtual compressor power (VCP) sensor, the virtual cooling capacity sensor, and the virtual COP sensor. To measure the refrigerant-side temperatures, a low-cost buffered analog-to-digital thermistor circuit was designed. The thermistors selected for the application can be easily surface-mounted to the RTU refrigerant circuit in the locations required. In comparison to other types of temperature sensors (thermocouples, RTDs, etc.) thermistors offer a good combination of accuracy, reliability, and cost. When using thermistors, the highly nonlinear relationship between temperature and internal resistance must be considered during the design process. While there are different ways to address this problem, each with their own tradeoffs, a more expensive (yet still relatively inexpensive) analog-to-digital converter (ADC) with a higher resolution was selected for this application.

Table 2.1. Description of required refrigerant-side temperature sensors used for RTU AFDD methods.

Symbol	Type	Description
T_{eri}	10 kΩ Thermistor[1]	Evaporator Refrigerant Inlet Temperature
T_{suc}	10 kΩ Thermistor	Compressor Refrigerant Suction Temperature
T_{crs}	10 kΩ Thermistor[2]	Condenser Refrigerant Saturation Temperature
T_{cro}	10 kΩ Thermistor	Condenser Refrigerant Outlet Temperature

[1] In some applications, a compressor suction pressure measurement is available. When this is the case, the T_{eri} sensor is not required since the evaporating temperature can be calculated using two-phase property relations.

[2] In some applications, a compressor discharge pressure measurement is available. When this is the case, the T_{crs} sensor is not required since the condensing temperature can be calculated using two-phase property relations.

It should also be noted that pressure measurements can be used to calculate the evaporator refrigerant inlet temperature and condenser refrigerant saturation temperature since the refrigerant at these points is a two-phase fluid. When this is the case, the saturation temperature and pressure are not

independent with their relationship determined by an equation of state. Systems that already have these pressure sensors installed for control purposes do not need to install additional temperature sensors which reduces the additional instrumentation costs for the proposed system. It is also worth noting that pressure sensors may be required for systems with micro-channel condensers. Locating a consistent and reliable saturation temperature point over the expected equipment operating range is not trivial task for these systems.

Low Cost Computing Device

Besides sensors and signal conditioning circuitry, the data-acquisition (DAQ) system requires a computational engine that is able to monitor the sensor outputs and perform the required mathematical transformations. The BeagleBone Black is a low-cost, open-source, community supported development platform with a TI Sitara™ ARM® Cortex A8 microprocessor that is capable of running the Linux operating system. In other words, the BeagleBone Black is a computer with all the components (microprocessor, RAM, hard drive, etc.) on a single circuit board. The first role of the BeagleBone Black in this application is to provide analog and digital interfaces between the DAQ software and the required sensors installed on the RTU. Compared to other microcontrollers and microprocessors, application development using the BeagleBone Black is easier since many of these low-level hardware and software interfaces are provided out of the box. The second role of the BeagleBone Black is to provide an interface for the virtual sensor outputs to be communicated with other applications (like the VOLTTRON platform) or users. The BeagleBone Black is not the only system capable of this; other development platforms are available with similar functionality. Development using the BeagleBone Black was selected since the TI Sitara™ microprocessor is widely available. Because of this, any work done with the prototype platform is almost directly translatable to any future platform using a similar chipset.

2.2 Initial Prototype and Testing

Using the sensor requirements described in Table 2.1, electronics system designs were developed that measured all the required state points. The actual design is shown in Figure B.1 of the Appendix. A cost study was performed in order to determine estimated component costs of the prototypes. An initial prototype of the virtual sensor system has been designed and built using actual electronics hardware, shown in Figure 2.1. The hardware selected for the prototype is generally considered to be typical and relatively low-cost when compared to similar data acquisition applications within the HVAC market. The prototype was also designed to simplify assembly and debugging so a few components not typically found in an actual application are used, namely the solderless breadboard (which can easily be swapped with a more permanent through-hole perforated board or printed circuit board) and the microprocessor development platform.

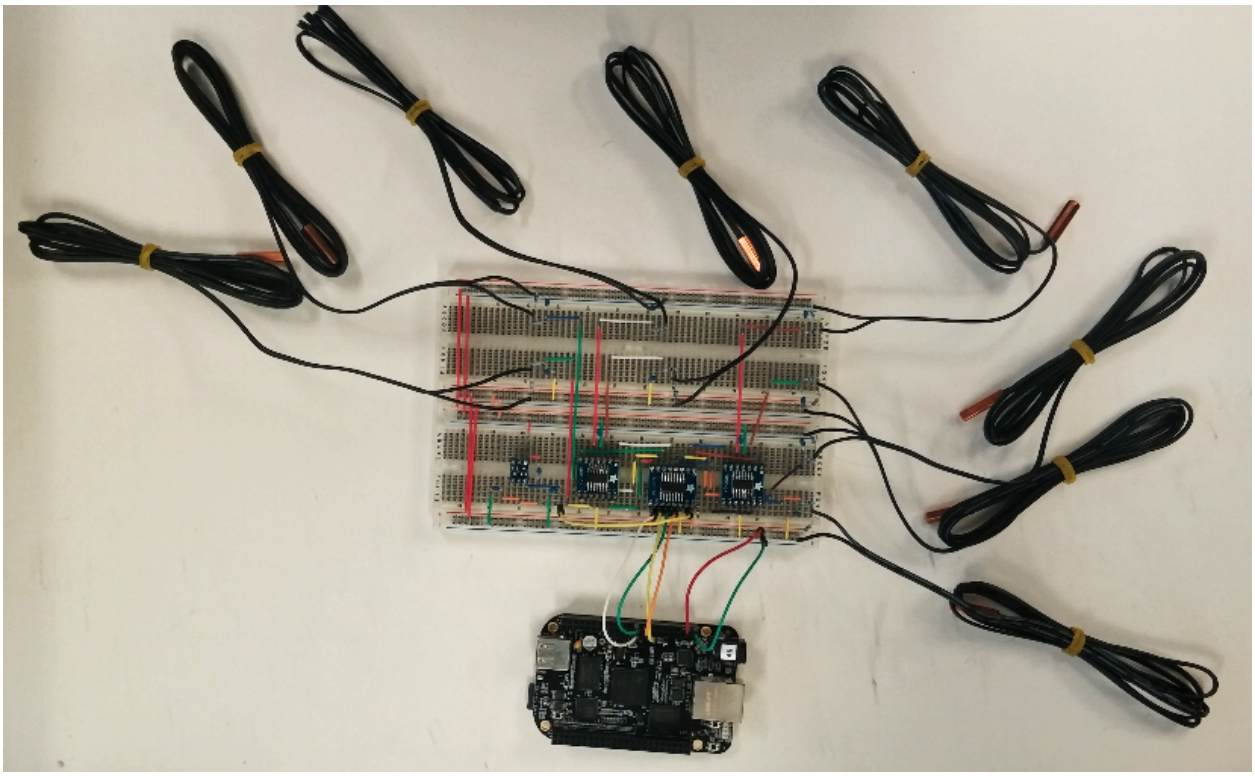

Figure 2.1. Virtual sensor package breadboard prototype hardware including the BeagleBone Black development platform and thermistor temperature sensors (additional thermistor inputs shown are part of the VOLTTRON RTU AFDD system developed for Project 2.2).

2.3 Initial Hardware Cost Study

Using actual costs of the required components from an electronics distributor, the component cost of the designed prototype was determined. In addition, an estimation of how much the component costs could be reduced by scaling up production was performed using the distributor's costs at larger quantities. The result of this study is shown in Figure 2.2 for different number of units manufactured. Figure 2.2 shows that significant component cost reductions (20-25%) can be realized when larger quantities are produced. The study also showed that the BeagleBone Black development platform is not a good component for an actual application since the price remained a constant $55.00 for all quantities of production. This is expected since the device is intended for prototyping and not for an actual product. To estimate the actual cost of a system, the TI Sitara™ microprocessor used in the BeagleBone Black was priced at different quantities and an additional 20% was added to account for other required components for the low-level interface implementations.

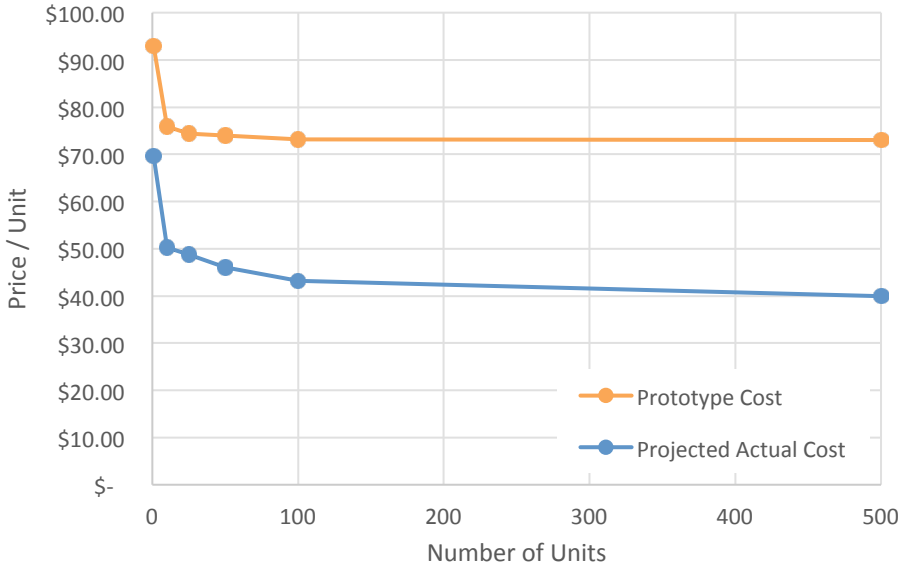

Figure 2.2. Projected virtual sensor system prototype component costs based on distributors' component cost at different quantities of production.

The initial cost study presented shows that the designed system has promise for future commercial production due to the relatively low component costs. It must also be noted that this study is not complete; only the component costs were detailed. Additional costs to manufacture the systems, as well as engineering and development costs must be accounted for. Nonetheless, this is a positive first step in the development of a commercial ready RTU AFDD system.

3. Description of Virtual Sensor System Software

The virtual sensor system software has been implemented using the Python programming language. Python offers several advantages over other programming languages, including development ease and speed, implicit code organization, and many scientific computing packages. All packages used in the RTU AFDD system are open-source and freely available. The VOLTTRON™ platform has also been implemented using Python, which further eases integration of the virtual sensor system into the VOLTTRON™ platform and the RTU AFDD system developed as part of Project 2.2.

The DAQ agent software is used to interface with the installed sensors for data processing. The sensor outputs are polled periodically using digital interfaces provided by the BeagleBone Black device. The thermistor temperature sensors are polled via the serial peripheral interface (SPI) on the BeagleBone Black that is connected to a 12-bit analog-to-digital converter. At a software configurable frequency, the DAQ agent emits time-stamped measurements via JSON encoded messages. A more detailed overview of this DAQ process is shown using a flow chart in Figure 3.1.

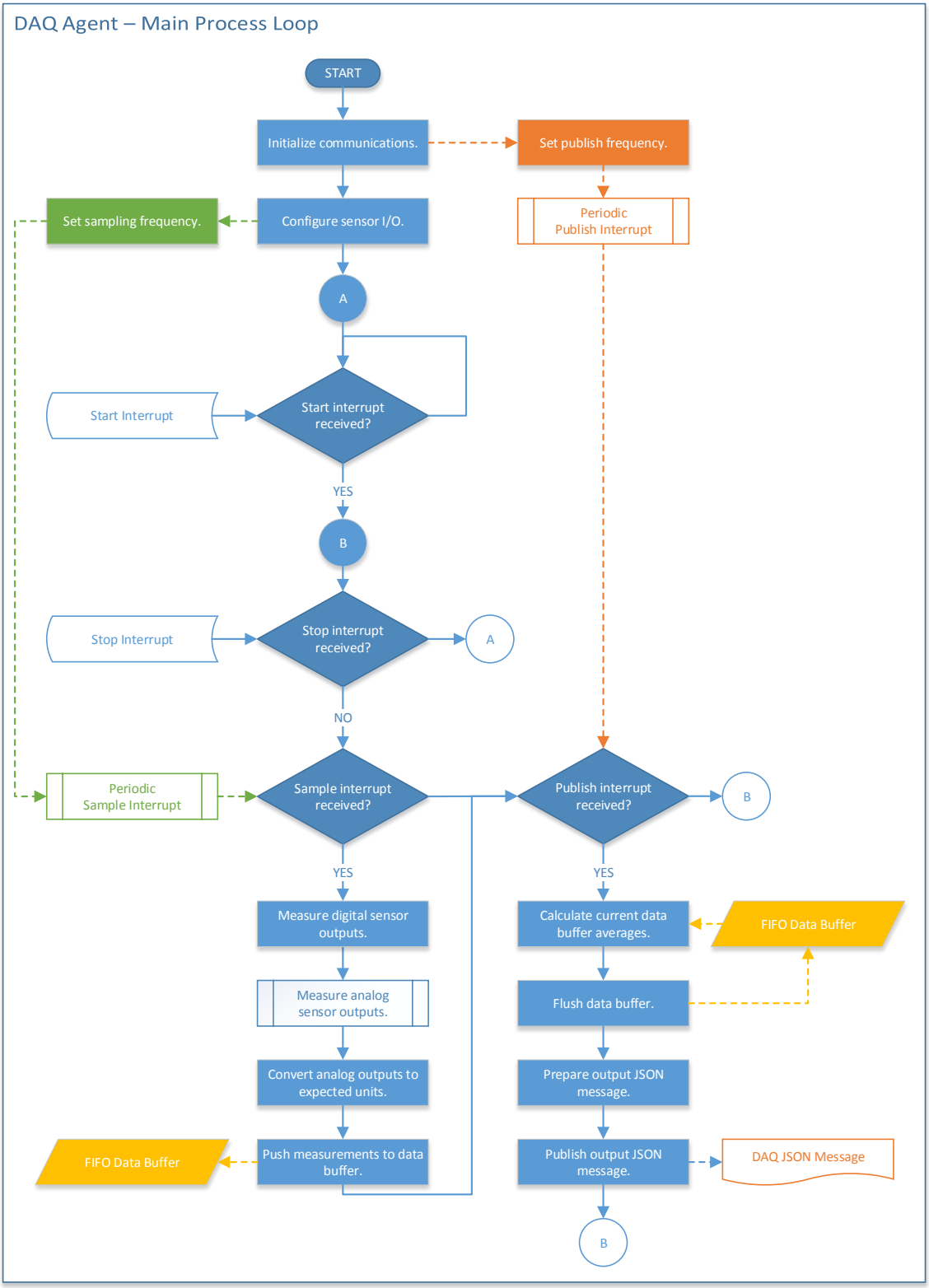

Figure 3.1. Flow chart depicting the main procedure used by the DAQ system to measure sensors used by the virtual sensor system.

Whenever a DAQ agent measurement message is emitted, the virtual sensor system receives the message. The virtual sensor agent uses the measurements to evaluate each virtual sensor model described in Section 1.2. Because of this, tuned virtual sensor parameters must be set on initialization using a JSON encoded configuration file. Like the DAQ agent, the virtual sensor agent produces a JSON encoded message containing the virtual sensor model outputs.

Two main processes are evaluated when a DAQ message is received. First, thermodynamic properties of each RTU system state point are determined. This includes determining saturation temperatures or saturation pressures and the enthalpy of different refrigerant state points. After the required thermodynamic properties have been determined, each virtual sensor output is determined. A more detail description of this process is shown in Figure 3.2.

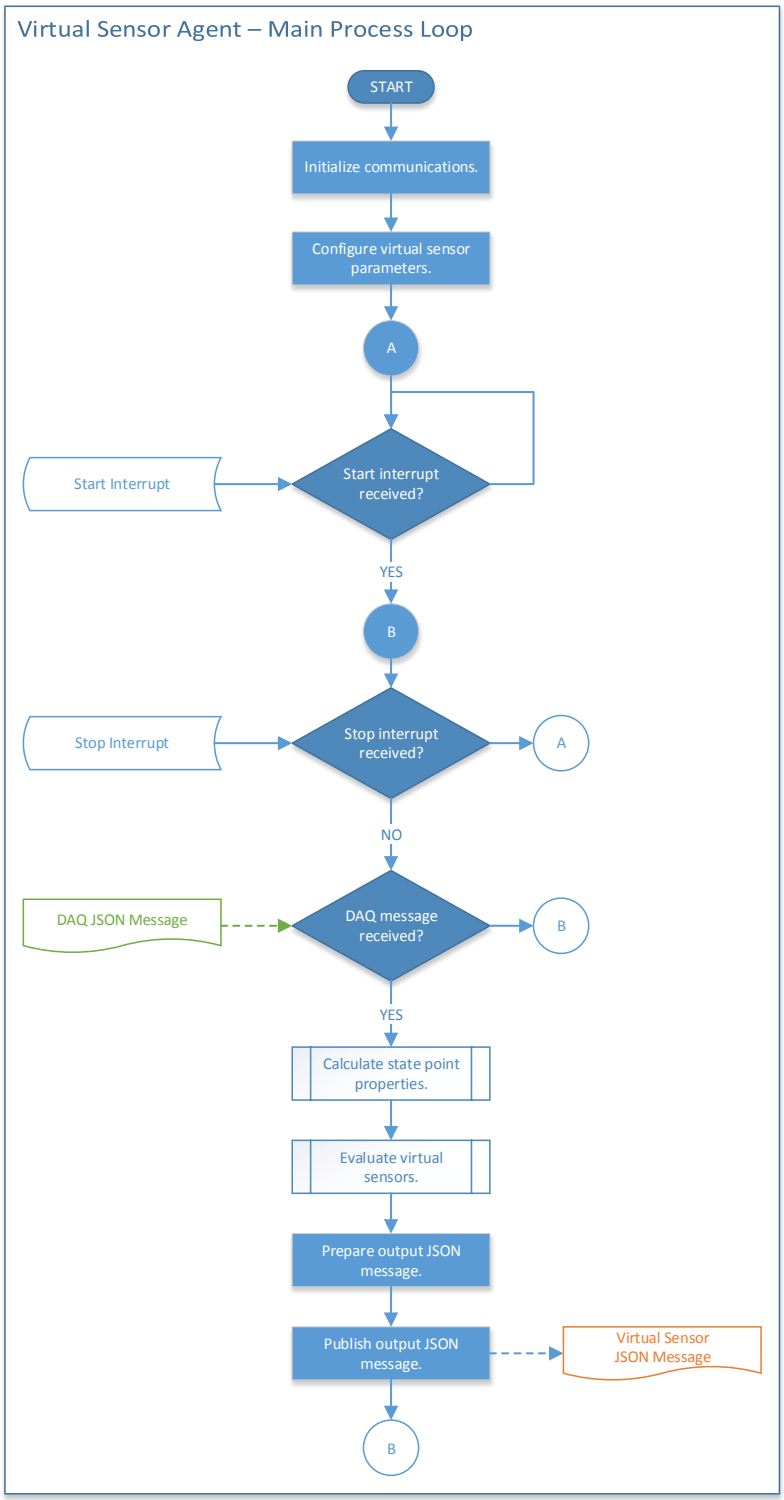

Figure 3.2. Flow chart depicting the main procedure used by the virtual sensor system to evaluate virtual sensor models using DAQ system outputs.

4. Laboratory Testing Plans

In order to test the performance of the automated VRC sensor training algorithm and virtual sensor implementation, a series of tests have been planned. The test plan has two primary considerations in mind: evaluate how well the open laboratory training algorithm tunes the empirical VRC parameters and how well the VRC sensor performs for different types of systems. Additionally, the performance of the virtual cooling capacity and COP sensor will be evaluated using experimental test data. To do this, combinations of different expansion valves and condenser coils will be used in a 5-ton RTU with two cooling stages, variable speed indoor blower, and variable speed outdoor fan will be used, described in Table 4.1.

The first system (System A, which is the same system that was previously tested in BP4) uses a thermostatic expansion valve (TXV) and a microchannel condenser coil. For the next set of tests, the expansion device will be replaced with a fixed orifice (FXO) throttling valve (System B). The size of the FXO has been recommended by the RTU manufacturer to ensure representative operation. With the valve installed, the automated VRC training algorithm will be applied to the system in order to determine the empirical VRC parameters. After this, the unit will be installed in psychrometric chambers to test performance at different combinations of charge levels and ambient conditions.

Table 4.1. System configurations and testing environments planned to evaluate automated virtual sensor training algorithm and virtual charge sensor performance.

ID	Expansion Device	Condenser Coil	Test Environment
A2[1]	TXV	Microchannel	Psychrometric Chamber Testing
A1[1]	TXV	Microchannel	Automated Open Lab Training
B1[1]	FXO	Microchannel	Automated Open Lab Training
B2	FXO	Microchannel	Psychrometric Chamber Testing
C1[2]	FXO	Finned-Tube	Automated Open Lab Training
C2	FXO	Finned-Tube	Psychrometric Chamber Testing
D1[2]	TXV	Finned-Tube	Automated Open Lab Training
D2	TXV	Finned-Tube	Psychrometric Chamber Testing

[1] Tests were completed during BP4 or earlier in BP5.
[2] Testing for C1 and D1 will be performed inside the psychrometric chambers simulating an open laboratory space. This will be done in order to accelerate the tests by not having to remove the RTU from the psychrometric chamber facility once it has been installed.

After the System B tests have been completed, the microchannel condenser coil originally installed on the system will be replaced with a finned round-tube condenser coil (System C). The same set of tests used to test System B will be repeated for System C with a slight modification to the open laboratory testing. Instead of removing the system after it has been installed in the psychrometric chamber facility to do open laboratory testing, the system will remain in the psychrometric chamber. This has been chosen in order to accelerate the tests since considerable time must be spent installing and removing the system from the psychrometric chambers otherwise. Finally, the FXO will be replaced on System C with the original TXV (System D) and the tests will be repeated.

Table 4.2. Optimal sequence of test conditions used in automated virtual charge sensor training algorithm.

Test	Charge Level[1] [%]	Compressor Stage [-]	Indoor Fan Torque[2] [%]	Outdoor Fan Torque[3] [%]
1	60	LOW	60	30
2	60	LOW	60	50
3	60	LOW	60	70
4	60	LOW	40	70
5	60	LOW	20	70
6	60	HIGH	90	60
7	60	HIGH	90	80
8	60	HIGH	90	100
9	60	HIGH	70	100
10	60	HIGH	50	100
11	70	LOW	60	30
12	70	LOW	20	70
13	70	HIGH	50	100
14	70	HIGH	90	60
15	80	LOW	60	30
16	80	HIGH	90	60
17	90	LOW	60	30
18	90	HIGH	90	60
19	100	LOW	60	30
20	100	HIGH	90	60
21	110	LOW	60	30
22	110	LOW	20	70
23	110	HIGH	50	100
24	110	HIGH	90	60
25	120	LOW	60	30
26	120	LOW	60	50
27	120	LOW	60	70
28	120	LOW	40	70
29	120	LOW	20	70
30	120	HIGH	90	60
31	120	HIGH	90	80
32	120	HIGH	90	100
33	120	HIGH	70	100
34	120	HIGH	50	100

[1] Charge is measured relative to the recommended charge according to the manufacturer's nameplate data.
[2] Indoor fan torque is set according to a nominal flow rate of 1350 CFM for low stage operation and 2000 CFM for high stage operation.
[3] Outdoor fan torque is set using the manufacturer's default values for low and high stage operation.

When the automated open laboratory VRC training algorithm is applied to the RTUs, operational state of the RTU is controlled to 34 different combinations of charge level, cooling stage, indoor fan torque, and outdoor fan torque. Each of these test combinations are shown in

Table 4.2. Despite having 34 test conditions, the entire sequence is expected to finish within 8-12 hours, though this will be optimized as testing progresses.

In order to validate the results of the automated VRC training procedure, extensive psychrometric chamber testing will be utilized. The aim of these tests is to evaluate the VRC sensor performance over a wide range of refrigerant charge levels and ambient conditions. The combinations of test conditions are shown in Table 4.3 and Table 4.4 for low stage cooling and high stage cooling respectively. The difference between testing at low stage cooling and high stage cooling involves the ambient conditions as well as the indoor and outdoor fan torque settings. For the low stage tests, cooler ambient conditions and reduced airflow rates are used to test the RTU. For the high stage tests, warmer ambient conditions and higher airflow rates are used to test the RTU.

Table 4.3. Psychrometric chamber testing conditions used to validate automated virtual charge sensor parameter tuning and virtual sensor performance for low cooling stage operation.

Test Variable		Test Values
Compressor Stage	[-]	LOW
Indoor Dry Bulb	[°F]	80
Indoor Wet Bulb	[°F]	67
Outdoor Dry Bulb	[°F]	69, 82, 95
Charge Level[1]	[%]	60, 70, 80, 90, 100, 110, 120
Indoor Fan Torque[2]	[%]	40, 60
Outdoor Fan Torque[3]	[%]	50, 70

[1] Charge is measured relative to the recommended charge according to the manufacturer's nameplate data.
[2] Indoor fan torque is set according to a nominal flow rate of 1350 CFM for low stage operation.
[3] Outdoor fan torque is set using the manufacturer's default value for low stage operation.

Table 4.4. Psychrometric chamber testing conditions used to validate automated virtual charge sensor parameter tuning and virtual sensor performance for high cooling stage operation.

Test Variable		Test Values
Compressor Stage	[-]	HIGH
Indoor Dry Bulb	[°F]	80
Indoor Wet Bulb	[°F]	67
Outdoor Dry Bulb	[°F]	82, 95, 108
Charge Level[1]	[%]	60, 70, 80, 90, 100, 110, 120
Indoor Fan Torque[2]	[%]	70, 90
Outdoor Fan Torque[3]	[%]	70, 100

[1] Charge is measured relative to the recommended charge according to the manufacturer's nameplate data.
[2] Indoor fan torque is set according to a nominal flow rate of 2000 CFM for high stage operation.
[3] Outdoor fan torque is set using the manufacturer's default value for high stage operation.

Generally, for open laboratory testing, one full week is allotted to collect results for each system. For psychrometric chamber testing, 4 weeks is allotted for each system (the testing for System A was completed in BP4). This schedule has periods allotted for component replacements and installation in the psychrometric chambers built in as well.

5. Preliminary Test Results

Experimental data has been collected to characterize the VRC sensor training algorithm applied to the 5-ton RTU with micro-channel condenser and TXV. A comparison of the VRC sensor applied to the open laboratory training data and psychrometric chamber test data for low cooling stage and high cooling stage are shown in Figure 5.1 and Figure 5.2, respectively. The results show that the open lab training system produces data that is representative of the psychrometric chamber data (which simulates actual operation). The VRC sensor performs better when the system is operated in high stage cooling mode. This may be due to more consistent superheat and subcooling when the system is run in high stage. Despite this, the VRC sensor had an overall root mean square error of 7.1%.

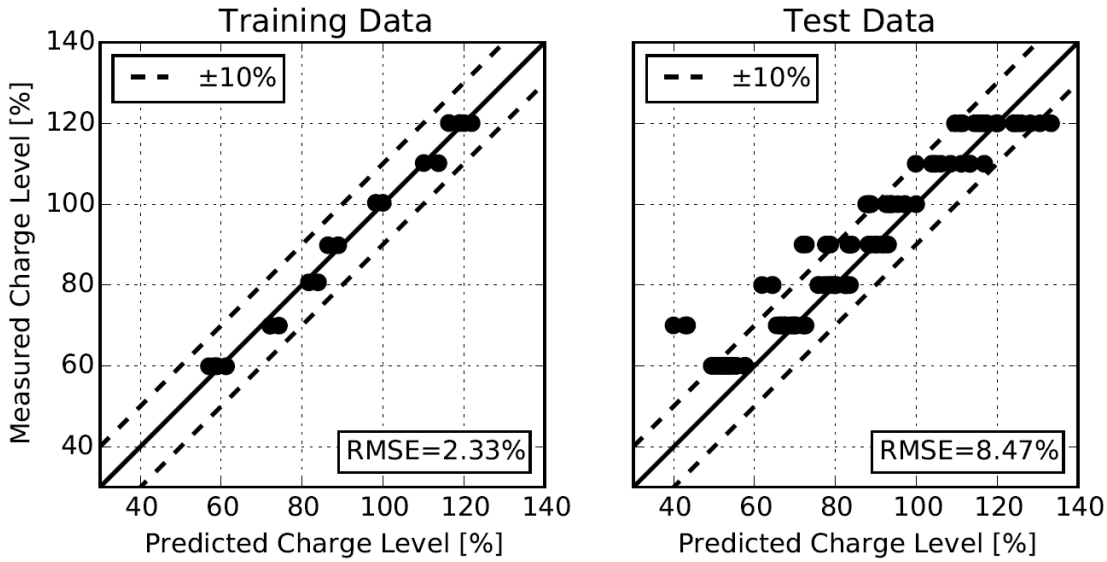

Figure 5.1. System A (micro-channel condenser, TXV) at low stage cooling operation comparison of training data error and test data error of the virtual refrigerant charge sensor least squares regression model using open laboratory data for training and psychrometric chamber test data for testing.

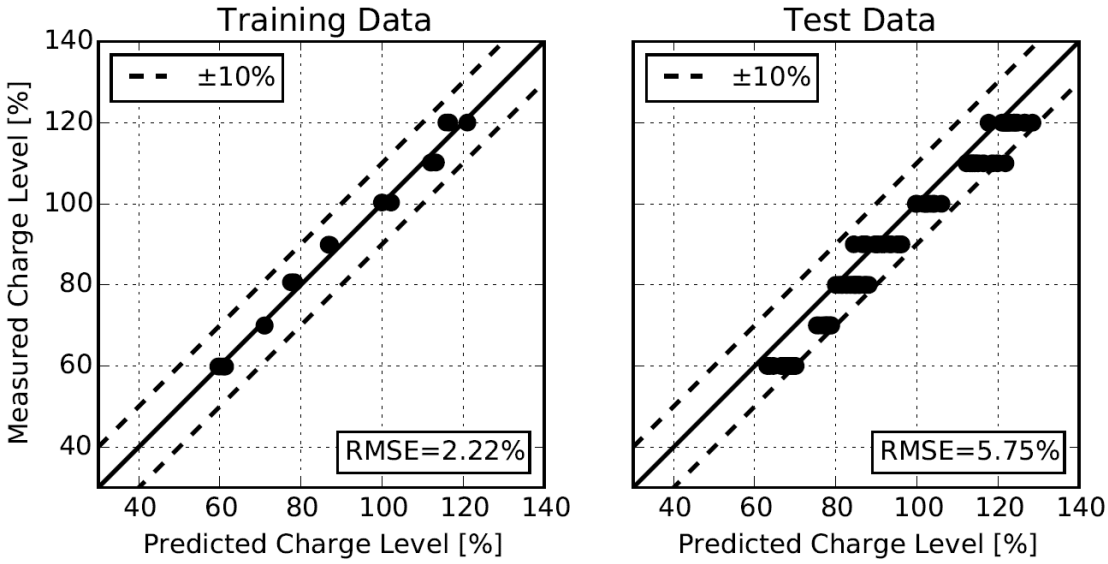

Figure 5.2. System A (micro-channel condenser, TXV) at high stage cooling operation comparison of training data error and test data error of the virtual refrigerant charge sensor least squares regression model using open laboratory data for training and psychrometric chamber test data for testing.

Using the VRC sensor algorithm, the virtual sensor system was applied to data collected from the psychrometric test data. Figure 5.3 shows the performance of the VRC sensor applied to a test case where the actual charge level in the system was 80% of the nominal level. The VRC system was able to accurately estimate the charge level of the system with relatively low variance. Figure 5.4 shows the charge fault impact for this system on capacity and COP. This impact was calculated as the ratio of the actual capacity or COP determined with virtual sensors to the normal capacity or COP determined using models of normal performance. This data shows that when the system is undercharged by 20% at a 95 °F ambient temperature, the system operates with approximately 9% less capacity and 4% less COP.

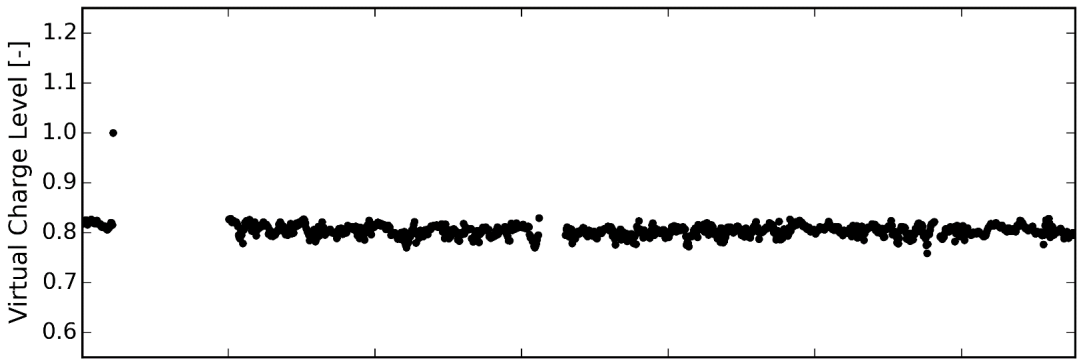

Figure 5.3. Virtual refrigerant charge sensor trended output for psychrometric chamber test data collected when System A had 80% of the nominal charge contained in the system.

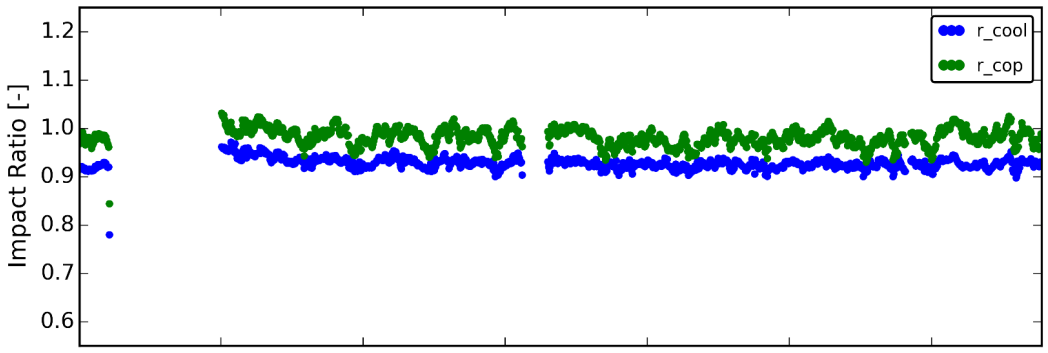

Figure 5.4. Cooling capacity impact (r_cool) and COP impact (r_cop) calculated using virtual sensor outputs and normal performance models trended for psychrometric chamber test data collected when System A had 80% of the nominal charge contained in the system.

After the expansion valve in the original RTU was replaced by a FXO, the virtual charge sensor training algorithm was reapplied to the system. Figure 5.5 and Figure 5.6 shows the training data error of the VRC sensor applied to the open laboratory data. These data show that the VRC model adequately estimates charge at different charge levels at both stages of operation. Tests are ongoing to collect experimental data from this RTU in psychrometric test chambers to assess whether the VRC sensor accurately predicts refrigerant charge level during actual operation.

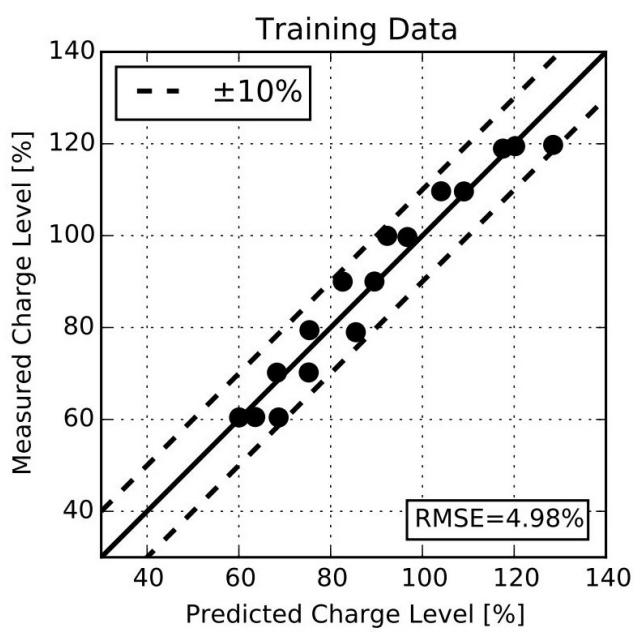

Figure 5.5. System B (micro-channel condenser, FXO) at low stage cooling operation training data error of the virtual refrigerant charge sensor least squares regression model using open laboratory data for training.

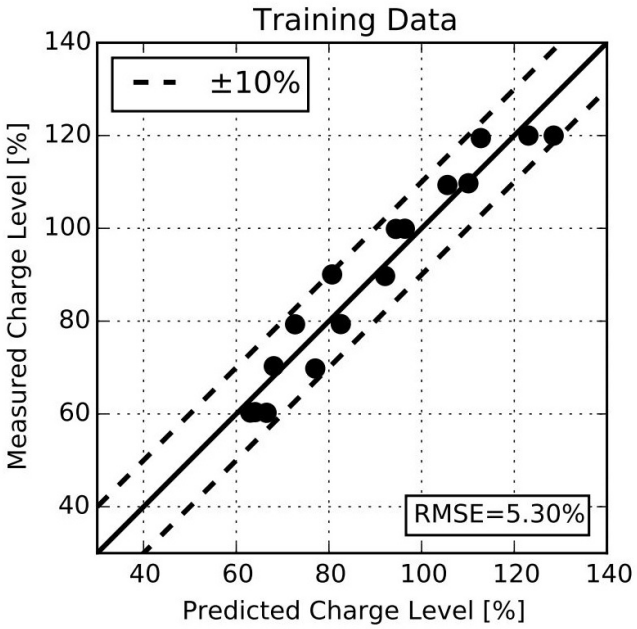

Figure 5.6. System B (micro-channel condenser, FXO) at high stage cooling operation training data error of the virtual refrigerant charge sensor least squares regression model using open laboratory data for training.

6. Conclusions

The hardware and software required to implement a fully functioning automated virtual refrigerant charge sensor training kit for open laboratory tested has been designed and documented. The design consists entirely of components that are easily acquired and software that is free and open source. Using these designs, a manufacturer could reduce the training time and cost requirements for virtual refrigerant charge sensor tuning. Plans have also been presented that evaluate how well the open laboratory training algorithm tunes the VRC sensor for multiple types of RTUs with different types of expansion valves and condenser coils. These test plans include testing the systems in the open laboratory as well as in psychrometric chambers to evaluate VRC sensor performance under different charge levels and ambient conditions. The outcome of this work will be an extensive study into the efficacy of the automated VRC sensor tuning methodology and the effectiveness of the VRC sensor applied to different systems.

Appendices

A. Source Code Listings

Fully documented source code listings for the microcontroller and training kit algorithm will be available from a repository found at the following address: https://www.github.com/ahjortland/rtu_afdd_agents.

B. Electronics Design Schematic

CONSORTIUM for
BUILDING ENERGY
INNOVATION